

THE SLOAN BRIGHT ARCS SURVEY: DISCOVERY OF SEVEN NEW STRONGLY LENSED GALAXIES FROM $z = 0.66$ – 2.94

JEFFREY M. KUBO^{1,6}, SAHAR S. ALLAM^{1,6}, EMILY DRABEK¹, HUAN LIN¹, DOUGLAS TUCKER¹, ELIZABETH J. BUCKLEY-GEER¹,
H. THOMAS DIEHL¹, MARCELLE SOARES-SANTOS^{1,2}, JIANGANG HAO¹, MATTHEW WIESNER³, ANDERSON WEST⁴, DONNA KUBIK¹,
JAMES ANNIS¹, AND JOSHUA A. FRIEMAN^{1,5}

¹ Center for Particle Astrophysics, Fermi National Accelerator Laboratory, Batavia, IL 60510, USA

² Instituto de Astronomia, Geofísica e Ciências Atmosféricas, Universidade de São Paulo, Brazil

³ Department of Physics, Northern Illinois University, DeKalb, IL 60115, USA

⁴ The Illinois Math and Science Academy, Aurora, IL 60506, USA

⁵ Department of Astronomy and Astrophysics, Kavli Institute of Cosmological Physics, University of Chicago, Chicago, IL 60637, USA

Received 2010 September 16; accepted 2010 October 18; published 2010 November 8

ABSTRACT

We report the discovery of seven new, very bright gravitational lens systems from our ongoing gravitational lens search, the Sloan Bright Arcs Survey (SBAS). Two of the systems are confirmed to have high source redshifts $z = 2.19$ and $z = 2.94$. Three other systems lie at intermediate redshift with $z = 1.33$, 1.82 , 1.93 and two systems are at low redshift $z = 0.66$, 0.86 . The lensed source galaxies in all of these systems are bright, with i -band magnitudes ranging from 19.73 to 22.06. We present the spectrum of each of the source galaxies in these systems along with estimates of the Einstein radius for each system. The foreground lens in most systems is identified by a red sequence based cluster finder as a galaxy group; one system is identified as a moderately rich cluster. In total, SBAS has now discovered 19 strong lens systems in the SDSS imaging data, 8 of which are among the highest surface brightness $z \simeq 2$ – 3 galaxies known.

Key words: galaxies: high-redshift – gravitational lensing: strong

Online-only material: color figures

1. INTRODUCTION

Strong gravitational lenses allow for the detailed study of distant background galaxies through the magnification provided by lensing. Models of these systems also provide interesting constraints on the underlying foreground lens mass distribution which includes the distribution of dark matter. Beginning with the serendipitous discovery of the 8’oclock arc (Allam et al. 2007) we have initiated the Sloan Bright Arcs Survey (SBAS), a systematic search of the Sloan Digital Sky Survey (SDSS) imaging database to search for candidate strong lensed systems. The first confirmed system from our systematic search was dubbed “the Clone” (Lin et al. 2009), which was followed by the discovery of six other systems described in Kubo et al. (2009). More recently we reported the discovery of four high redshift $z = 2$ systems in Diehl et al. (2009). To date we have discovered a dozen strong lens systems by mining the existing SDSS imaging data.

In this Letter, we report on a set of seven new systems in the SDSS imaging data which we have confirmed to be bona fide strong lens systems. These systems were confirmed via spectroscopy using the Apache Point Observatory (APO) 3.5 m telescope in New Mexico or the Mayall 4 m telescope at Kitt Peak National Observatory. This Letter is organized as follows: candidate selection and follow-up spectroscopy are described in Section 2. In Section 3 we report the details of each system including preliminary mass models and in Section 4 we summarize our results. Throughout the Letter, we use a flat cosmology with $\Omega_M = 0.3$, $\Omega_\Lambda = 0.7$, and $H_0 = 100 h \text{ km s}^{-1} \text{ Mpc}^{-1}$.

2. DATA

2.1. Lens Search

We searched for candidate strong lens systems in the 8000 deg^2 of SDSS imaging data. Specifically we performed two systematic searches of the SDSS Data Release Five (Adelman-McCarthy et al. 2007) and Data Release Six (Adelman-McCarthy et al. 2008). Our first candidate list was generated using the SDSS Catalog Archive Server database. Two separate queries were performed in which we searched for blue objects around a catalog of luminous red galaxies (LRGs; Eisenstein et al. 2001) and a catalog of brightest cluster galaxies (BCGs) generated using the maxBCG optical cluster finder algorithm (Hansen et al. 2005). Systems were then separated into groups depending on the number of blue objects, n , around each LRG or BCG. Each group of candidates was then visually examined by four different inspectors and flagged if they exhibited an arc-like morphology. The most promising systems were then chosen for follow-up. Our query for $n \geq 3$ objects produced a list of 1081 candidates, and one confirmed system discovered in this search is presented in Section 3.

Our second list is generated by performing a search against a catalog of merging galaxies generated using the method outlined in Allam et al. (2004). A merging galaxy pair is defined here as two galaxies in the range $16.0 < g < 21.0$ which are separated by less than the sum of their respective Petrosian radii (Stoughton et al. 2002). We ran this algorithm on imaging data from the SDSS DR6 and visually examined and classified the resulting catalog. A total of 5739 candidates were flagged by the algorithm, and upon visual inspection a list of 2761 objects were flagged as possible strong lens candidates. In Section 3, we report on six systems that have been followed

⁶ Equal first authors

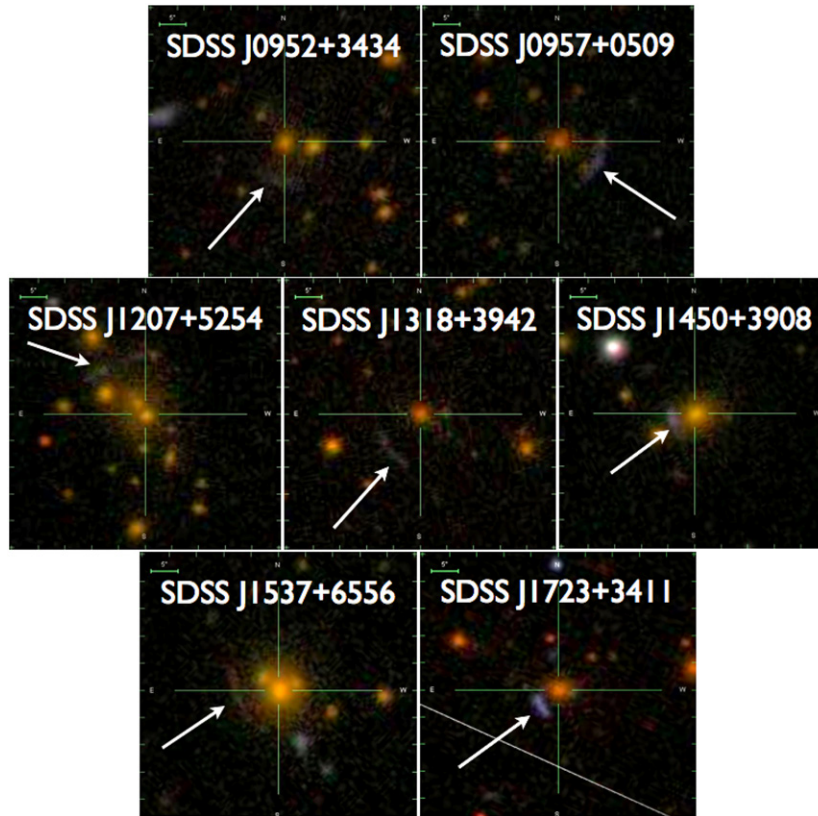


Figure 1. Mosaic of seven new strong lens systems discovered in the SDSS. Images are taken from the SDSS database. Systems are centered on the brightest LRG in each system. In each image north is up, east is to the left.

(A color version of this figure is available in the online journal.)

up from this list which we have confirmed to be strongly lensed galaxies.

2.2. APO Spectroscopy

Candidate systems were followed up with the Dual Imaging Spectrograph III (DIS) on the Apache Point Observatory 3.5 m telescope. DIS is a medium dispersion double spectrograph that has separated red and blue channels. The standard B400/R300 grating setup was used, which covers a spectral range of 3600–9600 Å. The dispersion is $1.83 \text{ Å pixel}^{-1}$ in the blue and $2.31 \text{ Å pixel}^{-1}$ in the red. We targeted each of our seven arcs with a typical exposure time of $3 \times 900 \text{ s}$. We used a $1''.5$ or $2''.0$ slit oriented along the brightest segment of the arc in order to maximize the signal-to-noise ratio. The data were reduced using standard IRAF tasks which we described previously in Lin et al. (2009) and Diehl et al. (2009). Redshift measurements were done using the *xcsao* task in the IRAF external package RVSAO (Kurtz & Mink 1998) by cross-correlation (Tonry & Davis 1979) against galaxy templates. For the templates, we used the composite Lyman break galaxy (LBG) template of Shapley et al. (2003) to cross-correlate against our higher-redshift source galaxies, and we used the galaxy templates from the SDSS DR2 template set⁷ (specifically template numbers 23–28, spanning the range of early- to late-type galaxies) for our lens galaxies and our lower-redshift source galaxies.

2.3. Kitt Peak Spectroscopy

We also followed-up one system, SDSS J0952+3434, with the RC Spectrograph (RCSpec), a low to moderate resolution spectrograph on the Mayall 4 m telescope at Kitt Peak National Observatory. We observed this system in long slit mode (with slit width of $1''.8$) and used the KPC-10A grating and the WG-345 order block filter to cover a wavelength range of about 3500–7500 Å (with a dispersion of $2.75 \text{ Å pixel}^{-1}$). The total exposure time was 4860s ($3 \times 900 \text{ s}$ and $3 \times 720 \text{ s}$). Data for this system were also reduced with standard IRAF tasks.

3. LENS SAMPLE

The seven new strong lens systems are shown in Figure 1. Each system has a dominant LRG and bluish arc located within an angular separation of $4''.4$ – $9''.4$ of the central LRG. To characterize the environment of each system we matched the lens coordinates against the gmBCG galaxy cluster catalog (Hao et al. 2010). The gmBCG algorithm (Hao et al. 2009) is a red sequence based cluster finding algorithm that calculates a gmBCG richness (N_{200}^{lens}) for each cluster, defined as the number of galaxies within a radius r_{200} centered on the BCG. The radius r_{200} is the radius in which the mass density falls to 200 times the critical density of the universe (Navarro et al. 1997). Six out of seven systems are matched to clusters in the gmBCG catalog, and each of the central LRGs is identified by the gmBCG algorithm as the BCG and also the central galaxy in each group. One of our lens systems (SDSS J0952+3434) is associated with a moderately rich cluster with $N_{200}^{\text{lens}} = 44$, while

⁷ <http://www.sdss.org/dr7/algorithms/spectemplates/index.html>

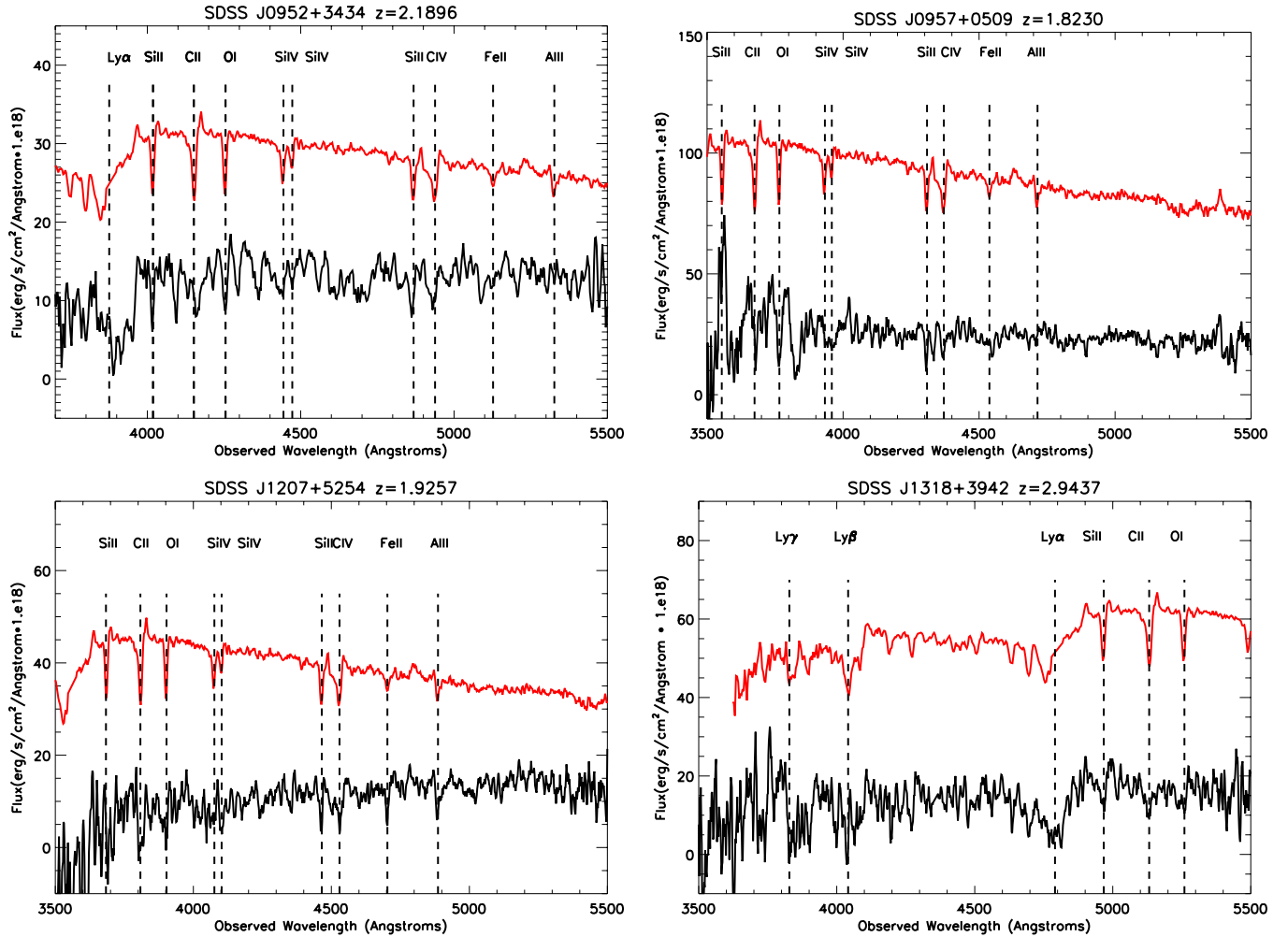


Figure 2. DIS spectra of the arcs in four systems are shown in black. Upper left: SDSS J0952+3434 has a redshift of $z = 2.1896$ (coadded DIS and RSpec data); upper right: SDSS J0957+0509 has $z = 1.8230$; lower left: SDSS J1207+5254 is at $z = 1.9257$; and lower right: SDSS J1318+3942 is at $z = 2.9437$. The DIS spectra are flux calibrated to f_λ units ($\text{erg s}^{-1} \text{cm}^{-2} \text{\AA}^{-1}$), but have also been multiplied by 10^{18} for plotting purposes. The red spectrum in each panel is the composite LBG template (Shapley et al. 2003) redshifted to match the arc in each case, and also arbitrarily rescaled and vertically offset for plotting purposes. The spectra of the arcs are discussed further in Section 3.

(A color version of this figure is available in the online journal.)

five other matching systems are associated with lower “group-scale” objects which lie in the richness range $7 < N_{200}^{\text{lens}} < 11$. The remaining system (SDSS J1537+6556) did not have a corresponding gmBCG richness measurement (see Section 3.6).

Because of the relatively poor image quality of the SDSS images (seeing $\sim 1''.3$), detailed models of our systems are not possible. Instead we adopt a simple model and describe each system with a singular isothermal sphere (Narayan & Bartelmann 1996). The resulting velocity dispersions fall in the range $501\text{--}707 \text{ km s}^{-1}$, which correspond to enclosed masses between $2.5 \times 10^{12} M_\odot$ and $10.5 \times 10^{12} M_\odot$. Magnitudes of the arc in each system are given in Table 1 and are in SDSS model magnitudes unless otherwise stated. In some cases the arc is split into multiple knots by the SDSS image deblender and in these cases the reported arc magnitude is the total sum of the individual knots. For one system (SDSS J1537+6556) the arc is not detected in the SDSS photometry, and we independently measure and report the isophotal magnitude with SExtractor (Bertin & Arnouts 1996). Below we briefly describe each system and present spectra for each arc shown in black in Figures 2 and

3. For comparison the composite LBG template⁸ or the SDSS galaxy template is shown in red, shifted to the same redshift of each source galaxy. A summary of all arc parameters is given in Table 1.

3.1. SDSS J0952+3434

SDSS J0952 + 3434 appeared in our search around BCGs and matches to a moderately rich galaxy cluster in the gmBCG cluster catalog with $N_{200}^{\text{lens}} = 44$. The lens consists of two LRGs with a blue arc located directly to the south. For the easternmost LRG ($r = 21.64$) we measure the spectroscopic redshift of the LRG to be $z = 0.3491 \pm 0.0001$. For the western LRG ($r = 19.51$) we measure a spectroscopic redshift of $z = 0.3598 \pm 0.0001$. Both LRGs are also members of the cluster as identified by the gmBCG algorithm. The blue arc is

⁸ Because none of our high-redshift source galaxies show $\text{Ly}\alpha$ in emission, we have interpolated over the strong $\text{Ly}\alpha$ emission line in the LBG template for both cross-correlation and plotting purposes. We apply this interpolation as it improves the significance of the cross-correlation peak when $\text{Ly}\alpha$ is present in the spectrum.

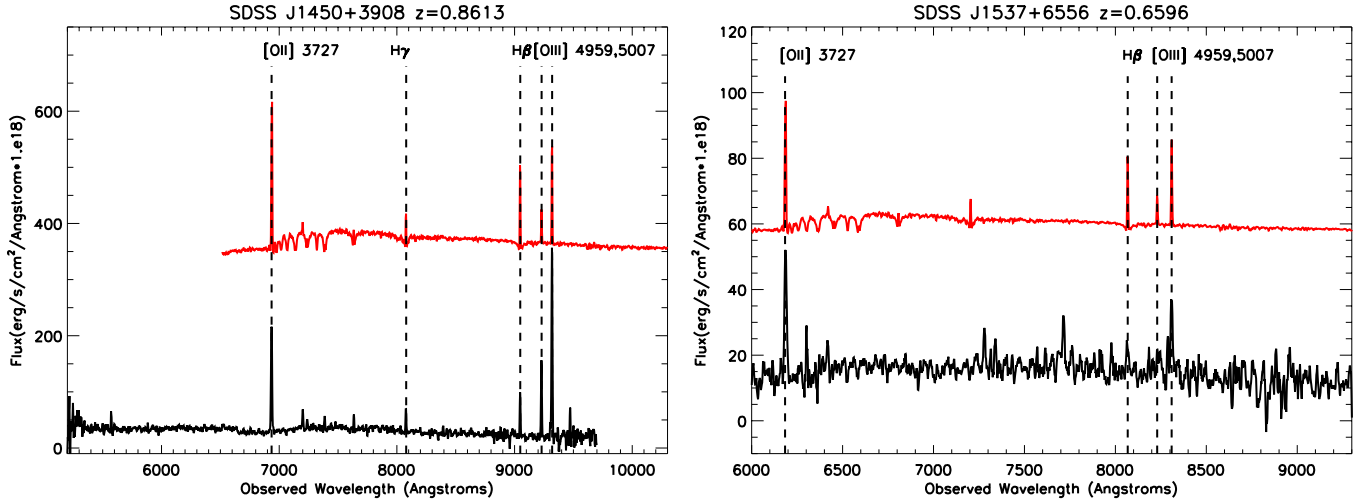


Figure 3. DIS spectra of the arcs in two systems (shown in black). Left: SDSS J1450+3908 has a redshift of $z = 0.8613$; and right: SDSS J1537+6556 is at $z = 0.6596$. The DIS spectra are flux calibrated to f_{λ} units ($\text{erg s}^{-1} \text{cm}^{-2} \text{\AA}^{-1}$), but have also been multiplied by 10^{18} for plotting purposes. The red spectrum in each panel is the SDSS emission-line galaxy template used for cross-correlation redshift measurements for these two arcs. The template has been redshifted to match the arc in each case, and also arbitrarily rescaled and vertically offset for plotting purposes. The spectra of the arcs are discussed further in Section 3.

(A color version of this figure is available in the online journal.)

Table 1
Parameters for Each Strong Lens System

System	R.A. (deg)	Decl. (deg)	z_l	z_s	θ_E^d (")	σ_v (km s^{-1})	$M(< \theta_E)$ ($10^{12} h^{-1} M_{\odot}$)	$(g, r, i)_{\text{arc}}$
SDSS J0952+3434	148.16760	34.57947	0.3491 ± 0.0001^b	2.1896 ± 0.0001^f	6.9	566 ± 12	5.6 ± 0.5	(21.52, 21.07, 21.01) ^c
SDSS J0957+0509	149.41330	5.15887	0.4469 ± 0.0002^b	1.8230 ± 0.0003^b	8.0	651 ± 12	9.8 ± 0.7	(20.55, 20.04, 19.73) ^c
SDSS J1207+5254	181.89964	52.91645	0.2717 ± 0.0002^b	1.9257 ± 0.0002^b	9.4	644 ± 10	8.2 ± 0.5	(20.81, 20.56, 20.01) ^c
SDSS J1318+3942	199.54796	39.70749	0.4751 ± 0.0002^a	2.9437 ± 0.0003^b	8.5	642 ± 11	10.5 ± 0.7	(21.04, 20.59, 20.24) ^c
SDSS J1450+3908	222.62770	39.13865	0.2893 ± 0.0002^a	0.8613 ± 0.0003^b	4.4	501 ± 17	2.5 ± 0.3	(21.50, 22.03, 22.06) ^c
SDSS J1537+6556	234.30500	65.93910	0.2595 ± 0.0001^b	0.6596 ± 0.0001^b	8.1	707 ± 13	8.3 ± 0.6	(22.46, 20.91, 20.19) ^e
SDSS J1723+3411	260.90067	34.19946	0.4435 ± 0.0002^b	1.3294 ± 0.0002^b	4.7	530 ± 17	3.8 ± 0.5	(20.77, 20.99, 21.09) ^c

Notes.

^a Spectroscopic redshift from the SDSS database.

^b Spectroscopic redshift determined using DIS on the APO 3.5 m.

^c Galaxy model magnitude (Stoughton et al. 2002) from the SDSS database.

^d Errors on manual fits to θ_E are estimated to be 0.3.

^e Isophotal magnitudes measured using SExtractor.

^f Spectroscopic redshift determined using data from DIS and RCSpec.

split by the SDSS imaging deblender into two knots, which combined give a total magnitude of $r = 21.07$. Along the arc we used data from both RCSpec and DIS to produce the coadded spectrum (total exposure time of 7560 s) shown in Figure 2. Cross-correlation against the LBG template yields a spectroscopic redshift of $z = 2.1896 \pm 0.0001$ for the arc. The spectrum plotted shows typical LBG absorption features due to Ly α , Si II, O I, C II, Si IV, and C IV. With a measured Einstein radius of $6''.9$, this corresponds to an enclosed mass of $(5.6 \pm 0.5) \times 10^{12} M_{\odot}$.

3.2. SDSS J0957+0509

SDSS J0957+0509 appeared in our merging galaxy catalog. The lens is a part of a small group of galaxies with $N_{200}^{\text{lens}} = 7$. The BCG in this group ($r = 18.85$) has a spectroscopic redshift determined from DIS to be $z = 0.4469 \pm 0.0002$ (not shown). A blue arc to the southwest is split into three knots which give an overall arc magnitude of $r = 20.04$. Along the arc we obtain the spectrum plotted in Figure 2, which shows typical, though relatively weak, LBG absorption features due to Si, C, and O, and we measure a cross-correlation redshift of

$z = 1.8230 \pm 0.0003$. With a measured Einstein radius of $8''.0$ this gives an enclosed mass of $(11.3 \pm 0.9) \times 10^{12} M_{\odot}$.

3.3. SDSS J1207+5254

SDSS J1207+5254 was flagged as a candidate in our merging galaxy catalog. The lens is a group of galaxies with $N_{200}^{\text{lens}} = 11$, with 2–3 LRGs interior to the arc. The brightest LRG ($r = 17.53$) has a spectroscopic redshift determined with DIS of $z = 0.2717 \pm 0.0002$ (not shown). This LRG was detected in the SDSS as one object, but based on the imaging may actually be two distinct LRGs. A third LRG interior to the arc is directed to the northeast with $r = 18.64$. An extended arc is located to the northeast of the central LRG and is also broken into several knots by the SDSS imaging deblender. The entire arc has a total magnitude of $r = 20.56$. Along the arc we obtain a spectrum that readily shows LBG absorption lines due to C II, O I, Si IV, Si II, C IV, Fe II, and Al II, and we find a cross-correlation redshift for the arc of $z = 1.9257 \pm 0.0002$ (Figure 2). With a measured Einstein radius of $9''.4$ this corresponds to an enclosed mass of $(8.3 \pm 0.5) \times 10^{12} M_{\odot}$.

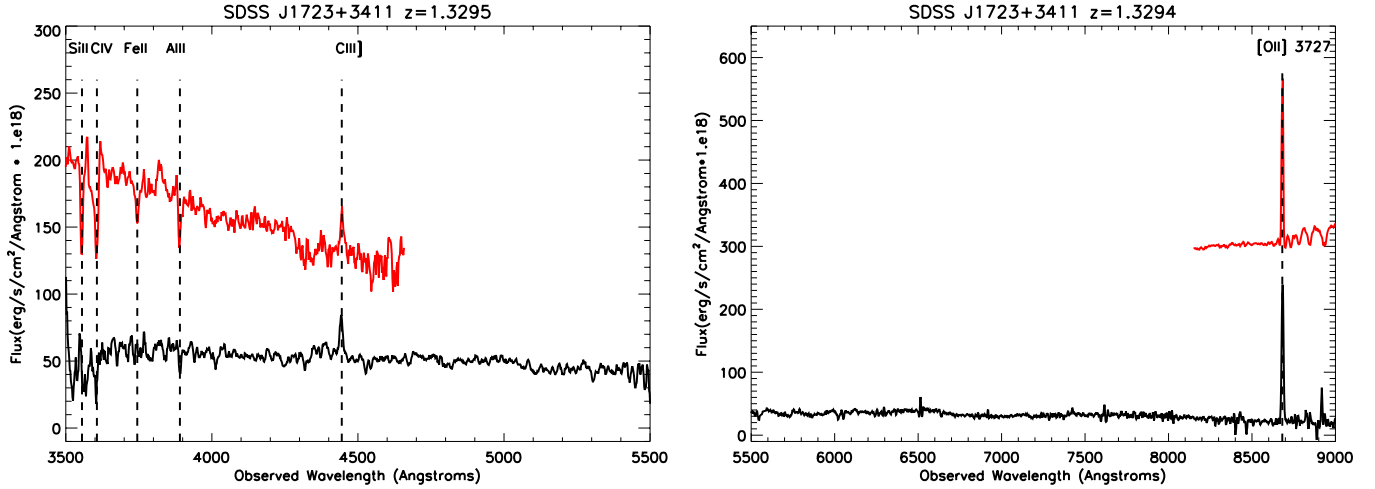


Figure 4. DIS spectra of the system SDSS J1723+3411 (shown in black). Left: the blue portion of the spectrum extending from 3500 Å to 5500 Å; and right: the red part of the spectrum extending from 5500 Å to 9000 Å. The DIS spectra are flux calibrated to f_λ units ($\text{erg s}^{-1} \text{cm}^{-2} \text{Å}^{-1}$), but have also been multiplied by 10^{18} for plotting purposes. The red spectrum in each case is the cross-correlation template used for that part of the spectrum, i.e., the composite LBG template in the blue, and an SDSS emission-line galaxy template in the red. The templates have been redshifted to match the arc in each case, and also arbitrarily rescaled and vertically offset for plotting purposes. Note the independently determined redshifts from the blue ($z = 1.3295 \pm 0.0002$) and red ($z = 1.3294 \pm 0.0002$) spectra are consistent with each other. The spectra are discussed further in Section 3.

(A color version of this figure is available in the online journal.)

3.4. SDSS J1318+3942

SDSS J1318+3942 was selected from our merging galaxy catalog. The lens is a group of galaxies ($N_{200}^{\text{lens}} = 10$) with a central LRG ($r = 18.82$) that has a spectroscopic redshift from the SDSS database of $z = 0.4751 \pm 0.0002$. To the southeast is a blue arc which has a total magnitude of $r = 20.59$. With DIS we identify strong $\text{Ly}\alpha$ absorption as well as other features due to Si II, C II, O I, $\text{Ly}\beta$, and possibly $\text{Ly}\gamma$ (Figure 2). Cross-correlation against the LBG template places the arc at a redshift of $z = 2.9437 \pm 0.0003$. We measure the Einstein radius of the system to be $\theta_E = 8''.5$ which gives an enclosed mass of $(10.5 \pm 0.7) \times 10^{12} M_\odot$.

3.5. SDSS J1450+3908

SDSS J1450+3908 was also selected from our catalog of merging galaxies. The foreground lens is a group ($N_{200}^{\text{lens}} = 8$) with an LRG ($r = 17.62$) that has a spectroscopic redshift from the SDSS DR7 database of $z = 0.2893 \pm 0.0002$. To the east of the LRG is a blue arc which is detected as a single object with $r = 22.03$. With DIS we measure five prominent emission lines [O II] 3727, [O III] 4959, [O III] 5007, $\text{H}\beta$, and $\text{H}\gamma$ (Figure 3) which place the arc at a redshift of $z = 0.8613 \pm 0.00003$. We measure the Einstein radius to be $\theta_E = 4''.4$, which corresponds to an enclosed mass of $(2.5 \pm 0.3) \times 10^{12} M_\odot$.

3.6. SDSS J1537+6556

SDSS J1537+6556 was selected from our merging galaxy catalog. The lens consists of a central LRG ($r = 16.91$) with two fainter galaxies embedded within the halo of the main LRG, one directed to the northeast, with $r = 20.77$, and the other directed to northwest, with $r = 19.09$. A blue extended arc is located to the east of the central LRG. This lens did not appear in the gmBCG catalog since it is located at the edge of the SDSS survey area. The SDSS photometric software did not converge on a magnitude for the arc so we have independently measured the arc's isophotal magnitude with SExtractor to be $r = 20.91$. For the central LRG, we measure a spectroscopic

redshift for the LRG using DIS to be $z = 0.2595 \pm 0.0001$ (not shown). We did not obtain redshifts for the two foreground galaxies associated with the central LRG. In the arc we measure four prominent emission lines: [O II] 3727, $\text{H}\beta$, [O III] 4959, and [O III] 5007, as shown in Figure 3, placing the arc at a redshift of $z = 0.6596 \pm 0.0001$. With a measured Einstein radius of $\theta_E = 8''.1$ the enclosed mass for this system is $(7.6 \pm 0.6) \times 10^{12} M_\odot$.

3.7. SDSS J1723+3411

SDSS J1723+3411 was selected from our merging galaxy catalog. The lens is a LRG ($r = 18.39$) for which we measure a spectroscopic redshift of $z = 0.4435 \pm 0.0002$ (not shown). The central LRG is identified by gmBCG as part of a small group with $N_{200}^{\text{lens}} = 8$. A blue arc ($r = 21.09$) is located to the southeast and we show both the blue and red parts of the DIS spectrum in Figure 4. In the blue part we see an emission line due to C III] 1908, along with possibly several weak LBG absorption features. In the red part of the spectrum we find a strong emission line due to [O II] 3727. Independent cross-correlations of the blue spectrum against the composite LBG template, and the red spectrum against an SDSS emission-line galaxy template (number 27), result in consistent redshift measurements, which we then combine to place the arc at a final redshift of $z = 1.3294 \pm 0.0002$. The measured Einstein radius of the system is $\theta_E = 4''.7$, which yields and enclosed mass of $(3.5 \pm 0.5) \times 10^{12} M_\odot$.

4. SUMMARY

We have presented seven new strong lens systems from SBAS, our ongoing search for strongly lensed galaxies in the SDSS imaging data. Two of these systems are of particular interest since they have source galaxies at high redshift, with $z = 2.9437$ and $z = 2.1896$. Because of magnification provided by lensing these are among the brightest galaxies known in this redshift range. The five remaining systems are source galaxies at intermediate and lower redshifts

$z = 1.9257, 1.8230, 1.3294, 0.8613, 0.6596$. To date SBAS has reported a total of 19 strong lens systems, 8 of which have source galaxies at high redshift $z \sim 2-3$. These bright, magnified galaxies are providing important windows into the star formation history and galaxy formation at high redshift. In upcoming papers, we will present detailed models of SBAS systems using high resolution *Hubble Space Telescope* imaging data as well as other ground-based follow-up data.

Fermilab is operated by the Fermi Research Alliance, LLC, under Contract No. DE-AC02-07CH11359 with the United States Department of Energy. These results are based on observations obtained with the Apache Point Observatory 3.5 m telescope, which is owned and operated by the Astrophysical Research Consortium. Funding for SDSS and SDSS-II has been provided by the Alfred P. Sloan Foundation, the Participating Institutions, the National Science Foundation, the U.S. Department of Energy, the National Aeronautics and Space Administration, the Japanese Monbukagakusho, the Max Planck Society, and the Higher Education Funding Council for England. The SDSS Web site is <http://www.sdss.org/>.

REFERENCES

- Adelman-McCarthy, J., et al. 2007, *ApJS*, **172**, 634
 Adelman-McCarthy, J., et al. 2008, *ApJS*, **175**, 297
 Allam, S. S., Tucker, D. L., Lin, H., Diehl, H. T., Annis, J., Buckley-Geer, E. J., & Frieman, J. A. 2007, *ApJ*, **662**, L51
 Allam, S. S., Tucker, D. L., Smith, J. A., Lee, B. C., Annis, J., Lin, H., Karachentsev, I. D., & Laubscher, B. E. 2004, *AJ*, **127**, 1883
 Bertin, E., & Arnouts, S. 1996, *A&AS*, **117**, 393
 Diehl, H. T., et al. 2009, *ApJ*, **707**, 686
 Eisenstein, D. J., et al. 2001, *AJ*, **122**, 2267
 Hansen, S. M., McKay, T. A., Wechsler, R. H., Annis, J., Sheldon, E. S., & Kimball, A. 2005, *ApJ*, **633**, 122
 Hao, J., et al. 2009, *ApJ*, **702**, 745
 Hao, J., et al. 2010, arXiv:1010.5503
 Kubo, J. M., Allam, S. S., Annis, J., Buckley-Geer, E. J., Diehl, H. T., Kubik, D., Lin, H., & Tucker, D. 2009, *ApJ*, **696**, 61
 Kurtz, M. J., & Mink, D. J. 1998, *PASP*, **110**, 934
 Lin, H., et al. 2009, *ApJ*, **699**, 1242
 Narayan, R., & Bartelmann, M. 1996, arXiv:astro-ph/9606001
 Navarro, J. F., Frenk, C. S., & White, S. D. M. 1997, *ApJ*, **490**, 493
 Shapley, A. E., Steidel, C. C., Pettini, M., & Adelberger, K. L. 2003, *ApJ*, **588**, 65
 Stoughton, C., et al. 2002, *AJ*, **123**, 485
 Tonry, J., & Davis, M. 1979, *AJ*, **84**, 1511